Coherent addition of gratings for chirped-pulse-amplified lasers based on near-field and far-field measurements

Yuchuan Yang (杨雨川)[1,2*], Hui Luo (罗 晖)[1], Xiao Wang (王 道)[2], Fuquan Li (李富全)[2], Xiaojun Huang (黄小军)[2], Bin Feng (冯 斌)[2], and Feng Jing (景 峰)[2]

[1] *College of Optic-Electric Science and Engineering, National University of Defense Technology, Changsha 410073, China*

[2] *Research Center of Laser Fusion, China Academy of Engineering Physics, Mianyang 621900, China*

[*] *Corresponding author: yyc_online@126.com*

Received October 12, 2010; accepted December 14, 2010; posted online March 28, 2011

The development of phased-array grating compressor is a crucial issue for high-energy, ultra-short pulse petawatt-class lasers. Almost all systems have adopted a tiled-grating approach to meet the size requirements for the compression gratings. We present a computer-control test system utilizing near-field interference and far-field focusing capable of monitoring and fast correcting tiled errors of the grating compressor. In this system, the tilt/tip errors between the two gratings are determined by the Fourier transform (FT) of the individual interference fringe, and the piston errors are determined by the ratio of the two primary peaks formed in the far-field pattern as a function of the piston difference. Monochromatic grating phasing is achieved experimentally and pulse compression is demonstrated with a tiled grating system.

OCIS codes: 140.7090, 320.5520, 050.1950.

doi: 10.3788/COL201109.041408.

The application of chirped pulse amplification (CPA) technique[1] to broadband, high-energy petawatt-class lasers implies the design of an efficient and large dimensional pulse compressor. Multilayer dielectric (MLD) gratings used in the pulse compressor are very promising in compressing high-energy pulses to the sub-picosecond regime. Due to the high diffraction efficiency, high damage threshold, good wavefront quality and large dimension, MLD gratings seem to be well-adapted[2,3]. However, these gratings are limited in size and cannot be used adequately for multi-kJ, short-pulse laser systems. To reach the petawatt regime with a compact pulse compressor, a grating phasing can be considered. The grating phasing consists of a coherent addition of multiple gratings that act as a large, monolithic grating[4].

The tiled compressors use spatially synchronous phase detection (SSPD) method to correct errors between the gratings. In this method, a closed-loop run, requiring correction of initial tip/tilt and piston errors, is completed in approximate 5 min[5,6]. The settling time depends on the severity of the initial misalignments. Given that gratings are dispersive devices, tiled gratings exhibit three additional degrees of differential errors: in-plane rotation (IPR), groove spacing, and lateral piston[7]. By controlling tip, tilt, and piston among the tiles, the gratings can thus be properly phased.

In this letter, we present a design proposal, which adjusts the tiled-grating surfaces to a phased wavefront generated by an interferometer and a far-field charge-coupled device (CCD) camera. Using this approach, segmented gratings have been aligned using near-field interferometers by sensing the tip, tilt, and the ratio of the two primary peaks formed in the far-field pattern by sensing piston.

The spatial interference intensity of two three-dimensional (3D) plane waves is described as

$$I(x,y,z) = I_1 + I_2 + 2E_1E_2\cos\delta(x,y,z), \qquad (1)$$

where

$$\delta(x,y,z) = (\mathbf{k}_{2x}-\mathbf{k}_{1x})x+(\mathbf{k}_{2y}-\mathbf{k}_{1y})y+(\mathbf{k}_{2z}-\mathbf{k}_{1z})z, \quad (2)$$

$\mathbf{k}_1$, $\mathbf{k}_2$ are the wave vectors of the two plane waves, respectively, I_1, I_2 are the light intensities of two plane waves, and E_1, E_2 are the electric field intensities. And the interference fringes are 3D uniformly-spaced parallel planes group. The tilt angle and closeness of parallel fringes are given as

$$\frac{\Delta y}{\Delta x} = \frac{\mathbf{k}_{2x}-\mathbf{k}_{1x}}{\mathbf{k}_{2y}-\mathbf{k}_{1y}},\ d_{\mathrm{f}} = \frac{\Delta x\Delta y}{\sqrt{(\Delta x)^2+(\Delta y)^2}}, \qquad (3)$$

where Δx and Δy are the spacing intervals of adjacent bright fringes along the x and y axes, respectively. $\Delta y/\Delta x$ and d_{f} indicate the tilt angle and closeness of parallel fringes respectively, which correspond to the sidebands position by the Fourier transform (FT) of the interference fringe[8]. The tilt and tip errors between the two apertures are determined by the position difference of the sidebands. The details of the far-field pattern formed by the subaperture are sensitive to the physical step between the two segments; the analysis presented below shows the process of measuring piston error[9].

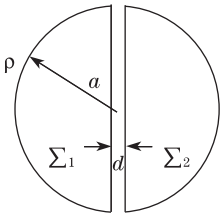

Fig. 1. Geometry of the limiting aperture.

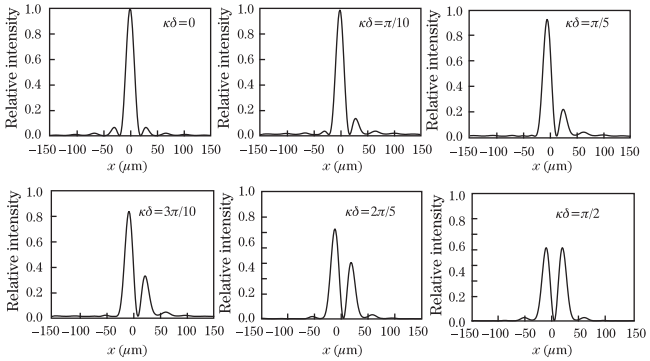

Fig. 2. Theoretical diffraction patterns (λ=0.6328 μm) for a split circular subaperture of radius a=4 cm and d=5 mm with a physical step δ between the two halves given by $k\delta$=0, $\pi/10$, $\pi/5$, $3\pi/10$, $2\pi/5$, and $\pi/2$.

We let $\boldsymbol{\rho}$, with circular coordinates (ρ, θ) (in units of length) be the position vector in the subaperture plane, and let $\boldsymbol{\omega}$ with circular coordinates (ω, ψ) be the position vector in the image plane. We consider a circular subaperture of radius a symmetrically straddling two segments divided by a gap (Fig. 1); the right ($\eta \geq d/2$) and left ($\eta \leq -d/2$) segments have piston errors of $\delta/2$ and $-\delta/2$, respectively. In addition, δ is the physical step height, and the corresponding wave-front step height is 2δ. The light is taken to be monochromatic with wavelength λ.

In the absence of other aberrations, the complex amplitude in the image plane $f(\boldsymbol{\omega}; k\delta)$ is simply the FT of the (complex) subaperture function $f(\boldsymbol{\rho}; k\delta)$[10]:

$$f(\boldsymbol{\rho}, k\delta) = \begin{cases} \exp(-\mathrm{i}k\delta) & \eta \geq d/2, \quad \boldsymbol{\rho} \leq a \\ \exp(\mathrm{i}k\delta) & \eta \leq -d/2, \quad \boldsymbol{\rho} \leq a \\ 0 & \rho > a \end{cases}, \tag{4}$$

$$f(\boldsymbol{\omega}; k\delta) = \frac{1}{\pi a^2} \iint\limits_{\sum_1} \exp(\mathrm{i}k\delta) \exp(\mathrm{i}k\rho \cdot \omega) \rho \mathrm{d}\rho \mathrm{d}\theta + \frac{1}{\pi a^2} \iint\limits_{\sum_2} \exp(-\mathrm{i}k\delta) \exp(\mathrm{i}k\rho \cdot \omega) \rho \mathrm{d}\rho \mathrm{d}\theta, \tag{5}$$

where k=$2\pi/\lambda$ and the normalization is chosen, such that the on-axis, in-phase intensity is unity (see below). The aperture cross effects are incorporated into the data analysis.

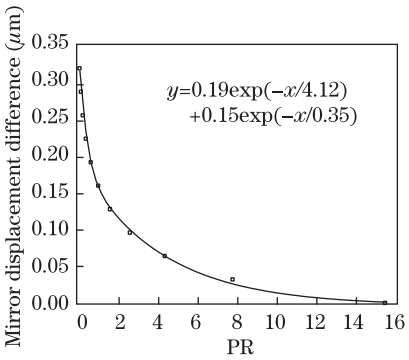

Fig. 3. PR calibration curve of Fig. 2.

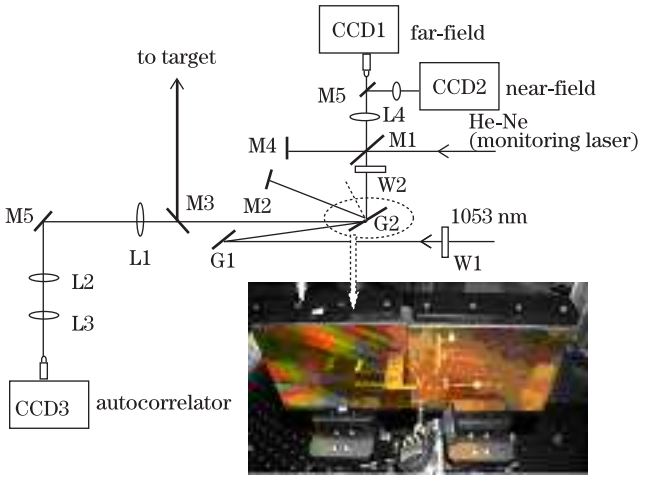

Fig. 4. Optical schematic of monitoring laser path with the phased grating compressor and tiled grating entity (seen the below)

The algorithm used to extract phase information from a single intersegment piston step was applied. Based on the diffraction theory, the algorithm exploited the diffraction pattern produced by a small intersegment subaperture and monochromatic light from the detect source. The resulting simulated diffraction patterns of projection on the x axis for various piston steps are shown in Fig. 2.

The approach to extract the phase was based on extracting a single characteristic value from each simulated image related to piston step and then calculating a calibration curve from it. The characteristic value, which was applied here, was the ratio between the two main peaks in the diffraction pattern (Fig. 2). This technique is commonly referred to as the peak ratio technique, with

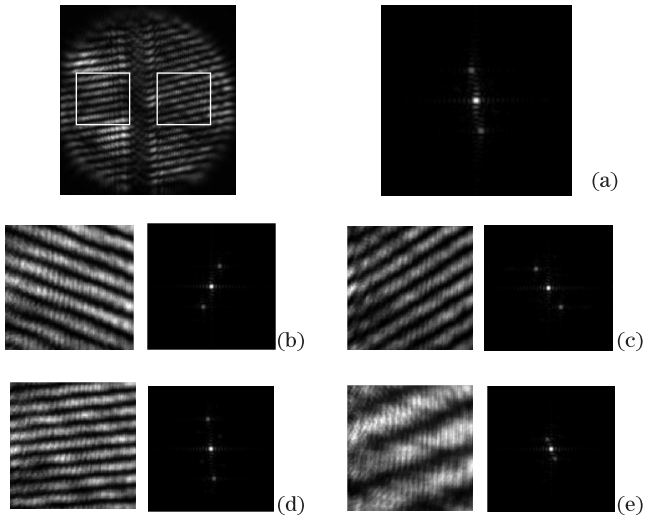

Fig. 5. FT-based algorithm used to analyze fringe patterns with tiling errors. (a) Image captured by CCD (left) and the FT result of the fringes in the left-half frame (right), (b)–(e) typical fringe patterns and corresponding FT results by adjusting the stepping motors.

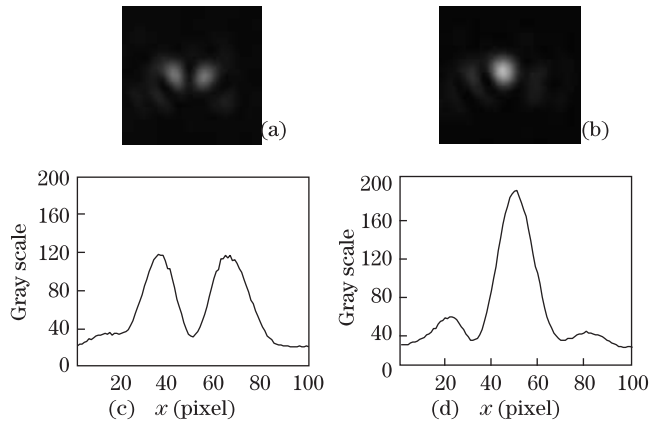

Fig. 6. Far-field patterns captured by CCD camera. (a) Symmetrically splitting focal spot for $k\delta = (1/2 + n)\pi$, (b) ideal focal spot for $k\delta = \pi$, (c) and (d) are corresponding light intensity distribution of Figs. 6(a) and (b) at vertical center along horizontal, respectively.

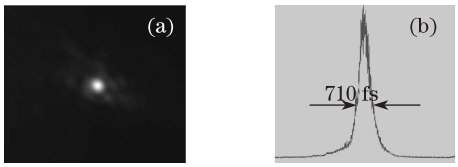

Fig. 7. (a) Far-field pattern of the main laser and (b) the autocorrelation trace of the compressed pulse.

strong anti-noise and fast calculation advantages[11]. Defining the peak ratio (PR) as PR = Max (left peak)/Max (right peak), we obtain the calibration curve (Fig. 3). In Fig. 3, the first-order exponential decay polynomial curve is fitted by PR from the simulation, and the maximum fitted error is less than 5 nm. For the given subaperture image in Fig. 1, the PR was calculated and processed with the fitted formula to obtain the required piston step or phase step.

Gratings position and grooves orientation have to be accurately controlled to provide a phased-array grating compressor. Therefore, we have developed a mechanical system to phase two medium-scale diffraction gratings (G2 in Fig. 4). Several motion devices allow up to five degrees of freedom between the two 420×210 (mm) MLD diffraction gratings manufactured by Jobin-Yvon.

The experimental bed used to demonstrate monochromatic grating phasing was configured in the vacuum compressor chamber, in which an He-Ne monitoring laser operated at 632.8 nm. The beam size of the monitoring laser expanded to Φ 100 mm was centered on the gratings gap through splitter M2 and window W2 (Fig. 4). A 20 cm-diam on-gauge plate (M4) was then used to reflect reference light, and a 5 cm-diam beam splitter mirror (M5) was inserted to simultaneously monitor the far-field (f=0.578 m) and near-field patterns. The main laser was injected from window W1 before being relayed to a pulse compressor consisting of G1, G2, and M2 before reaching the focusing parabola in the target chamber. Afterwards, the light leakage from M3 was used to measure the pulse duration.

Figure 5 presents the process of adjusting tilt/tip errors using the fringe matching technique with near-field interference fringes. The left half-side interference fringes in Fig. 5(a) are taken as reference mark, while the right half-side interference fringes are adjusted to match this using the stepping motors. The tilted angle and closeness of parallel fringes correspond to the deviation of either sidebands along the horizontal and normal directions. The central position of the sidebands was then determined by the centroid method, whose minimum resolution approached 0.5 μm (CCD pixel: 4.7 × 4.7 (μm), improving by almost 10×); thus, the tilt/tip errors were confined within 1 μrad.

Once the tilt and tip are corrected in real time, the remaining piston errors could be removed using the PR technique. According to the calibration curve in Fig. 3, the corresponding piston movement was then applied on the grating subaperture, after which the monochromatic grating phasing was realized and maintained easily by closed-loop control. As can be seen, the piston accuracy is nearly 60 nm limited by stepping motors (the Piezoelectric transition (PZT) driver further improves the tiled precision effectively). Figure 6(a) shows a piston phase error of $\lambda/2$, which can be calculated by PR (≈1, Fig. 6(c)), and the good alignment is reached by adjusting corresponding movement in Fig. 6(b), in which the peak ratio is 4.36 (the piston error is 62 nm).

Figure 7 shows the far-field pattern of the main laser operating at 1.053 μm, which has been transferred to the pulse compressor and an autocorrelation trace of a compressed pulse obtained with a tiled grating. As can be seen, the main laser size and energy transferred to the pulse compressor are 28.5 × 28.5 (cm) in area and 144 J through main amplifiers; the focal spot full-width at half-maximum (FWHM) size in Fig. 7(a) is 23 μm (1.3× diffraction limit) and the pulse duration is 710 fs in Fig. 7(b). The spectral width of the CPA output is about 4 nm after main amplifiers, while the chirping ratio is 4 nm/ns, so the compressibility is more than 1.4×10^3.

In conclusion, we have demonstrated a tiling grating phase adjustment based on near-field and far-field monitoring in a compressor configuration, confirming the feasibility of grating tiling. The alignment errors within a tiled compressor have been compensated by adjusting tilt/tip-piston, and the decoupling of tilt/tip-piston has effectively shortened the adjusting time compared with the SSPD method. A chirped pulse amplification system with a phased-array grating compressor has been performed to compress several hundred Joule pulses, after which the pulse width is measured to be less than 1 ps. Nevertheless, some grating setting accuracy improvements are necessary to yield better tiled performance.

This work was supported by the National "863" Program of China (No. 2009AA8044005) and the Laboratory of Laser Fusion and Research Center of Laser Fusion under the Innovatory Fund (No. 20090604).

References

1. D. Strickland and G. Mourou, Opt. Commun. **56,** 219 (1985).
2. K Hehi, J Bischoff, U Mohaupt, M. Palme, B. Schnabel, L. Wenke, R. Bödefeld, W. Theobald, E. Welsch, R. Sauerbrey, and H. Heyer, Appl. Opt. **38,** 6257 (1999).

3. C. Li, J. Wu, X. Chen, Z. Hu, and G. Qian, Acta Opt. Sin. (in Chinese) **29,** 1943 (2009).
4. T. Zhang, M. Yonemura, and Y. Kato, Opt. Commun. **145,** 367 (1998).
5. A. Cotel, M. Castaing, P. Pichon, and C. Le Blanc, Opt. Express **15,** 2742 (2007).
6. J. Bunkenburg, T. J. Kessler, W. Skulski, and H. Huang, Opt. Lett. **31,** 1561 (2006).
7. T. J. Kessler, J. Bunkenburg, H. Huang, A. Kozlov, and D. D. Meyerhofer, Opt. Lett. **29,** 635 (2004).
8. S. Zhou, Y. Yang, W. Chen, W. Yan, P. Ma, W. Jiang, S. Hu, and X. Tang, Acta Opt. Sin. (in Chinese) **29,** 702 (2009).
9. G. Chanan, M. Troy, and F. Dekens, S. Michaels, J. Nelson, T. Mast, and D. Kirkman, Appl. Opt. **37,** 140 (1998).
10. M. Born and E. Wolf, *Principles of Optics* (6th ed.) (Pergamon, New York, 1969), pp. 395-398.
11. G. Chanan, C. Ohara, and M. Troy, Appl. Opt. **39,** 4706 (2000).